Chapter 3

Solution of fractional order reaction-advection-diffusion equation arising in Porous media

3.1 Introduction

By porous media, it is understood a physical system with voids. These pores are generally filled with fluids like gases or liquids. Porous media is a very useful concept in several areas of applied sciences like-filtration, geomechanics, construction, material sciences etc. By porous media we mean a solid which allows a passage of fluids through its voids and pores. Natural examples of porous media are- sand, limestone etc. Based on structure, porous media can be further characterised at two different geological levels i.e., microscopic level and macroscopic level. The former

The contents of this chapter have been published in **Journal of Porous Media**, (1), **22**(2018) S309-S316.

deals with expression of structure with the help of degree of inter-connection, orientation of pores etc. whereas the latter deals with bulk parameters, which have been averaged over scale much larger than the size of pores. Based on our objective, we can prefer any of the two approaches, but to have a basic understanding of surface phenomena such as absorption, it is clear that microscopic description is necessary. Several articles are available in literature which discuss different models on porous media [101], [102], [103], [104], [105], [106], [107], [108] and [109].

In most of the cases, pollutant movement in the subsurface is dominated by advection. It describes the pollutant transfer by the bulk movement of flowing groundwater. The movement of mass entrained in the flow is referred to as advection. Solute advection is the movement of dissolved substances due to the movement of the water in which they are suspended. Advection not only moves mass from one place to another, but it also distributes or scatters the matter. This happens because the distribution of water velocity is not uniform. The advection diffusion equation describes the transport of a solute under the combined effects of advection and diffusion. If the chemical being carried through soil is reactive, its behaviour in groundwater is described by reaction-advection-diffusion equation. Reaction term represents the source and the sink term in the advection-diffusion equation. The additional source term will increase whereas the sink term will lead to reduction in contaminant concentraion. Reduction due to degradation will be zero for the case of conservative contaminant.

Groundwater system or aquifer is a classical example of porous media. Contamination of groundwater is a severe problem for humans as its decontamination is an extremely difficult and costly affair. The near or sub-surface storage or disposal of waste such as septic tank sludge, grass waste, and industrial wastes is the primary cause of groundwater pollution. When the contaminants enter the aquatic subsurface environment, they move through an aquifer along with groundwater. The

fate of the contaminant in natural systems like dust pollution, river thermal pollution and groundwater contamination, may be modelled using partial differential equation (PDE) and more particularly, fractional-order PDE (FPDE) [95], [100], [93]. The movement of pollutants in the groundwater, atmosphere and surface water can be more accurately modeled mathematically by the fraction order reaction-advection-diffusion equation (FRADE).

The spatial and temporal profiles of pollutant concentration in the aquifer can be predicted by solving RADE with defined boundary and initial conditions. Because of numerous applications in diverse domains, such as physical, chemical, geological, biological, and financial systems, fractional calculus has received a lot of attention in recent years. A fractional-order diffusion mathematical model that describes non diffusive transportation in turbulence of plasma [110] and a nonlinear fractional order diffusion model for the flow in capillaries across porous media are just a few examples [111]. The mathematical models of physical systems have been observed to be more precise when fractional calculus is used. In both industry and academia, the use of fractional derivative as a tool to construct more stable mathematical models to study the complicated engineering problems are gaining popularity. When fractional-order derivatives are used instead of integer-order derivatives, a practical mathematical description of any physical phenomenon based on current and earlier time is produced. The microscopic dynamics of transportation of mass in porous media is extremely complicated, and the physical events have peculiar kinetics that the ordinary diffusion equation cannot account for, but the fractional diffusion equation does.

For contaminant transport in grounwater, fractional order ADE has shown great prospects in simulating the physical system in a better way as compared to integral order ADE. It has been reported by many researchers that the FRADE are much more effective than integer order RADE in simulating the flow and transport in

porous media [112], [113], [114]. For instance, [112] by comparison with observations concluded that for heterogeneous porous media, FRADE give more acurate results especially for longer transport distances. Moreover, FRADE simulated the tailing parts of breakthrough curves much better and accounted for the earlier arrival of tracer. Similarly, in [113] it is observed better matching of the results of their time fractional RADE with the experimental outcomes. [115] opined that the fractional mass conservation equation can represent the nonlinear flux with more accuracy than the first order linear Taylor series to account for the related heterogeneity.

The common removal mechanisms in groundwater systems include the presence of microorganisms capable of biodegrading certain compounds, physical decay and adsorption of the contaminant on the soil part of the aquifer. Biodegradation, an important aspect of contaminant flow, may be enhanced to remove contaminants. Adsorption, a retardation reaction between solute and surface of the porous structure, is an important factor in contaminant movement. It effects in segregating the hazardous compounds from the groundwater and also slowing the movement of the compound are remarkable. Solute transport phenomena with nonlinear biodegradation occur in many situations like contamination of inorganic chemical and metal in soil and groundwater systems [116], [117]. The contaminant under the condition of nonlinear degradation results into nonlinear differential equation in both integer order or fractional order system as described in the following mathematical model. As shown in [60] and [118], for contaminant migration in heterogeneous porous media and earth surfaces such as natural rivers, the fractional-order form of the RADE is advantageous. To solve the fractional-order transport equation in disordered semiconductors, fractional-order transport equation within Liouville equations is examined by [119]. Many scholars have contributed to the development of strategies for solving fractional order PDEs which are both reliable and efficient. In [120], a space

fractional order solute transport system is solved using finite difference method. The fractional order convection–diffusion equation arising in underground water pollution is solved using dual Bernstein operators in [121]. In [122], the Caputo-Fabrizio derivative is applied to groundwater flow within the confined aquifer. In this chapter, the following fractional order nonlinear RADE is considered as

$$\frac{\partial^{\alpha} u}{\partial t^{\alpha}} = D\frac{\partial^{2\beta} u}{\partial x^{2\beta}} + D\frac{\partial^{2\beta} u}{\partial y^{2\beta}} - \nu_1 \frac{\partial^{\beta} u}{\partial x^{\beta}} - \nu_2 \frac{\partial^{\beta} u}{\partial y^{\beta}} - \lambda u(1-u), \tag{3.1}$$

where $0 < \alpha \leq 1$, $0.5 < \beta \leq 1$, with the initial condition

$$u(x, y, 0) = \xi_1(x, y), \tag{3.2}$$

and boundary conditions as

$$u(0, y, t) = \xi_2(y, t), \tag{3.3}$$

$$\frac{\partial^{\beta} u(1, y, t)}{\partial x^{\beta}} = \xi_3(y, t), \tag{3.4}$$

$$\frac{\partial^{\beta} u(x, 0, t)}{\partial y^{\beta}} = \xi_4(x, t), \tag{3.5}$$

$$\frac{\partial u(x, 1, t)}{\partial y} = \xi_5(x, t), \tag{3.6}$$

where u is the function $u(x, y, t) \in C[0, 1] \times C[0, 1] \times C[0, 1]$, D is the diffusion coefficient and ν_1, ν_2 are the velocities of solute transport. $\frac{\partial^{\alpha} u}{\partial t^{\alpha}}, \frac{\partial^{2\beta} u}{\partial x^{2\beta}}$, $\frac{\partial^{2\beta} u}{\partial y^{2\beta}}$, $\frac{\partial^{\beta} u}{\partial x^{\beta}}$ and $\frac{\partial^{\beta} u}{\partial y^{\beta}}$ are all Caputo fractional order derivatives of $u(x, y, t)$.
Since exact solutions of nonlinear FPDEs are difficult to obtain, the numerical and approximate approaches are used to solve these equations. As discussed previously, numerical solutions utilising various advanced techniques are beneficial in dealing

with nonlinear situations. Since Legendre polynomials satisfy the orthogonality criterion, the Legendre collocation method with operational matrices is a trustworthy method for solving nonlinear FPDEs. During the solution of differential equations, the approach employs a truncated orthogonal series. Legendre operational matrices have been generalised to fractional-order derivative by [77].

3.2 Numerical Application

This section deals with the validation of the proposed method by applying it to two standard test cases where exact solutions are known. For the comparison of the approximate and the exact solutions, let us define the L^2- error in $0 \leq x \leq 1$ as

$$||u(x,1,1) - u_{n,n,n}(x,1,1)||_2 = \sqrt{\int_0^1 |u(x,1,1) - u_{n,n,n}(x,1,1)|^2 dx}, \tag{3.7}$$

where $u(x,y,t)$ and $u_{n,n,n}(x,y,t)$ represent the exact and approximate solutions, respectively.

The rate of convergence (ρ) is calculated using the formula

$$\rho = \lim_{k\to\infty} \frac{||u_{k+1,k+1,k+1}(x,1,1) - u(x,1,1)||_2}{||u_{k,k,k}(x,1,1) - u(x,1,1)||_2}. \tag{3.8}$$

The L^∞- error in $0 \leq x \leq 1$ is defined as

$$||u(x,1,1) - u_{n,n,n}(x,1,1)||_\infty = Sup\{|u(x,1,1) - u_{n,n,n}(x,1,1)|: x \in [0,1]\}. \tag{3.9}$$

3.2.1 Example [3]

Let us consider the following fractional order RADE as

$$\frac{\partial^\alpha u}{\partial t^\alpha} = D(\frac{\partial^\beta u}{\partial x^\beta} + \frac{\partial^\beta u}{\partial y^\beta}) - \nu(\frac{\partial u}{\partial x} + \frac{\partial u}{\partial y}) - \lambda u(1-u), 0 < \alpha < 1, 1 < \beta < 2, \quad (3.10)$$

where u is a function in $u(x, y, t) \in C[0, 1] \times C[0, 1] \times C[0, 1]$ with initial condition

$$u(x, y, 0) = (1 + exp(\frac{1}{\sqrt{6}}(x - \frac{y}{\sqrt{2}})))^{-2}, \quad (3.11)$$

and boundary conditions

$$u(0, y, t) = (1 + exp(\frac{1}{\sqrt{6}}(-\frac{y}{\sqrt{2}}) - \frac{5t}{\sqrt{6}}))^{-2}, \quad (3.12)$$

$$u(1, y, t) = (1 + exp(\frac{1}{\sqrt{6}}(1 - \frac{y}{\sqrt{2}}) - \frac{5t}{\sqrt{6}}))^{-2}, \quad (3.13)$$

$$u(x, 0, t) = (1 + exp(\frac{1}{\sqrt{6}}(x) - \frac{5t}{\sqrt{6}}))^{-2}, \quad (3.14)$$

$$u(x, 1, t) = (1 + exp(\frac{1}{\sqrt{6}}(x - \frac{1}{\sqrt{2}}) - \frac{5t}{\sqrt{6}}))^{-2}, \quad (3.15)$$

which has the exact solution [3]

$$u(x, y, t) = (1 + exp(\frac{1}{\sqrt{6}}(x - \frac{y}{\sqrt{2}}) - \frac{5t}{\sqrt{6}}))^{-2}. \quad (3.16)$$

To validate our proposed numerical method, it is applied to the above problem and the L^2 and L^∞ normed errors between the exact and obtained numerical solutions have been calculated. The results are shown through Table 3.1 for $n = 7, 8, 9, 10$, $D = 0.5 = \nu$, $\lambda = 1$ at $\alpha = 0.7, \beta = 1.7$.

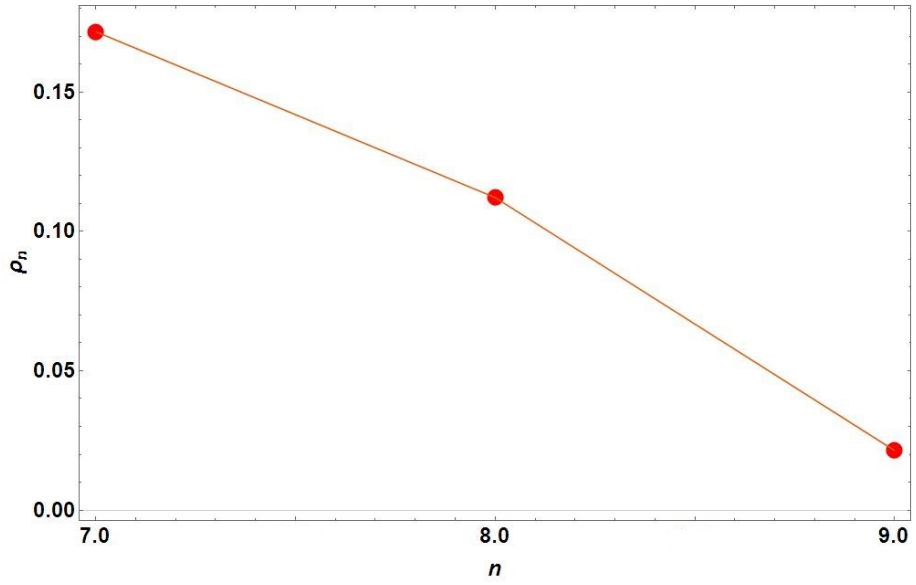

Figure 3.1: Plot of rate of convergence ρ_n against n for $n = 7, 8, 9$ in Example 1.

n	$\|\|u(x,1,1) - u_{n,n,n}(x,1,1)\|\|_2$	$\|\|u(x,1,1) - u_{n,n,n}(x,1,1)\|\|_\infty$
7	1.72555×10^{-6}	1.05859×10^{-5}
8	2.96011×10^{-7}	2.53432×10^{-6}
9	3.3182×10^{-8}	9.57486×10^{-7}
10	7.1009×10^{-10}	8.32516×10^{-8}

Table 3.1 L^2 and L^∞-errors between the approximate and the exact solutions for $n = 7, 8, 9, 10$ for Example 1.

It is seen that L^2 and L^∞ normed errors defined by (3.8) and (3.9) decrease as n increases. Table 3.1 clearly shows that the obtained numerical results by the proposed method are accurate even for small value of n.

The rate of convergence is defined by

$$\rho_n = \frac{||u_{n+1,n+1,n+1}(x,1,1) - u(x,1,1)||_2}{||u_{n,n,n}(x,1,1) - u(x,1,1)||_2}.$$

After computation, we get $\rho_7 = 0.1716$, $\rho_8 = 0.1121$ and $\rho_9 = 0.0214$. Here $\rho_7 > \rho_8 > \rho_9$ and $\rho_7, \rho_8, \rho_9 \in (0, 1)$.

Thus a sequence $\{\rho_n\}$ is obtained such that $\rho_n \to 0$ for sufficiently large n. Hence it

may be concluded that the convergence of our proposed method is superlinear. The Figure 3.1 also justifies the superlinear convergence of the method.

3.2.2 Example [4]

The proposed method is also applied to the following problem to show its accuracy and efficiency.

$$\frac{\partial^\alpha u(x,y,t)}{\partial t^\alpha} = (0.5)\Delta^2 u(x,y,t) + u(x,y,t)^2(1-u(x,y,t)) + f(x,y,t), \tag{3.17}$$

where

$$f(x,y,t) = e^{xy}(1.91116t^{1.1} + e^{xy}t^4(-1+e^{xy}t^2) - 0.5t^2(x^2+t^2)), \tag{3.18}$$

with initial condition

$$u(x,y,0) = 0, \tag{3.19}$$

and boundary conditions

$$u(0,y,t) = t^2, \tag{3.20}$$

$$u(x,0,t) = t^2, \tag{3.21}$$

$$u(1,y,t) = e^y t^2, \tag{3.22}$$

and

$$u(x,1,t) = e^x t^2. \tag{3.23}$$

The exact solution is given by [4],

$$u(x,y,t) = e^{xy}t^2. \tag{3.24}$$

The L^2 and $L^\infty-$ normed errors between the obtained results and the exact results are calculated for $n = 6, 7, 8, 9$, for $\alpha = 0.9$, which are displayed through Table 3.2. It is clear from Table 3.2 that the proposed numerical method is efficient even for smaller values of n.

As in previous example, we get $\rho_6 = 0.0309$, $\rho_7 = 0.02755$, $\rho_8 = 0.01119$ and again notice that $\rho_6 > \rho_7 > \rho_8$ and $\rho_6, \rho_7, \rho_8 \in (0, 1)$. Thus a sequence $\{\rho_n\}$ is obtained with $\rho_n \to 0$ as n becomes large which clearly concludes that the proposed method is superlinear, which is also justified by Figure 3.2.

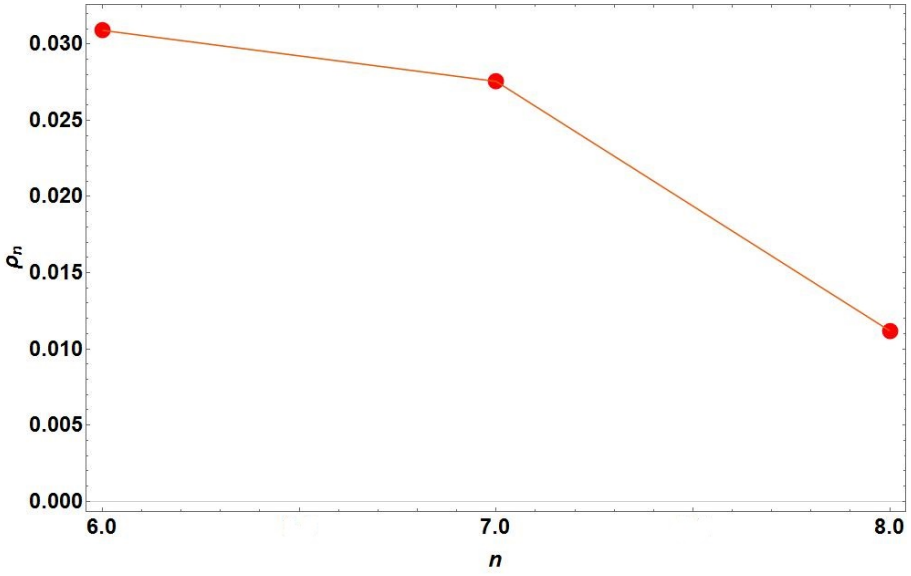

Figure 3.2: Plot of rate of convergence ρ_n against n for $n = 6, 7, 8$ in Example 2.

n	$\|\|u(x,1,1) - u_{n,n,n}(x,1,1)\|\|_2$	$\|\|u(x,1,1) - u_{n,n,n}(x,1,1)\|\|_\infty$
6	3.8141×10^{-8}	4.39728×10^{-8}
7	1.17892×10^{-9}	1.2757×10^{-9}
8	3.24816×10^{-11}	1.20232×10^{-10}
9	3.6379×10^{-13}	6.12022×10^{-11}

Table 3.2 L^2 and $L^\infty-$ errors between the approximate and the exact solutions for $n = 6, 7, 8, 9$ for Example 2.

It is also clear from the Table 3.2 that the errors are much lesser as compared to the method applied in [4]. Therefore, it may be claimed that the proposed method is superior than the existing method given in [4].

3.3 Solution of the problem

After validation of the proposed numerical method on two existing problems, it is employed to solve the considered fractional order RADE model (3.1) under the initial condition as

$$u(x, y, 0) = 1 \tag{3.25}$$

and boundary conditions as

$$u(0, y, t) = t, \tag{3.26}$$

$$\frac{\partial^\beta u(1, y, t)}{\partial x^\beta} = 0, \tag{3.27}$$

$$\frac{\partial^\beta u(x, 0, t)}{\partial y^\beta} = 0, \tag{3.28}$$

$$\frac{\partial u(x, 1, t)}{\partial y} = 0, \tag{3.29}$$

To solve this model let us first approximate the unknown function $u(x, y, t)$ defined in equation (1.47) as

$$(\psi_n(t))^T U(\psi_n(x) \otimes \psi_n(y)).$$

After substituting the approximation of unknown function $u(x, y, t)$ and using operational matrix of fractional order derivative defined in equation (1.48), and taking

everything on the left hand side and adding initial condition to this resulting equation, we get

$$\begin{aligned}(\psi_n(t))^T(D^{(\alpha)})U(\psi_n(x)\otimes\psi_n(y)) - D(\psi_n(t))^T U(D^{(2\beta)}\otimes I)(\psi_n(x)\otimes\psi_n(y))\\ - D(\psi_n(t))^T U(I\otimes D^{(2\beta)})(\psi_n(x)\otimes\psi_n(y))\\ + \nu_1(\psi_n(t))^T U(D^{(\beta)}\otimes I)(\psi_n(x)\otimes\psi_n(y))\\ + \nu_2(\psi_n(t))^T U(I\otimes D^{(\beta)})(\psi_n(x)\otimes\psi_n(y))\\ + \lambda(\psi_n(t))^T U(\psi_n(x)\otimes\psi_n(y))\\ - \lambda((\psi_n(t))^T U(\psi_n(x)\otimes\psi_n(y)))^2 = 0, \qquad (3.30)\end{aligned}$$

and the approximation of the boundary conditions are given by

$$(\psi_n(t))^T U(\psi_n(0)\otimes\psi_n(y)) - t = 0, \qquad (3.31)$$

$$(\psi_n(t))^T U(D_n^{(\beta)}\otimes I)(\psi_n(1)\otimes\psi_n(y)) = 0, \qquad (3.32)$$

$$(\psi_n(t))^T U(I\otimes D_n^{(\beta)})(\psi_n(x)\otimes\psi_n(0)) = 0, \qquad (3.33)$$

$$(\psi_n(t))^T U(I\otimes D_n^{(1)})(\psi_n(x)\otimes\psi_n(1)) = 0. \qquad (3.34)$$

Let us now collocate the equation (3.30) at points (x_i, y_j, t_k) and equations (3.31) to (3.34) at points (x_i, t_k) and at points (y_j, t_k), where x_i, y_j are Legendre-Gauss-Lobatto (LGL) points of the $L_{n-1}(x)$ and $L_{n-1}(y)$, respectively where $t_k's$ are the zeroes of the Shifted Legendre polynomial $L_{n+1}(t)$. After the collocation, the equations are converted to a linear system of algebraic equations from which the unknown matrix U can be obtained by using Newton method. Substituting the matrix U, the approximate solution of $u(x, y, t)$ will be obtained.

Figure 3.3 depicts the movement of solute concentration due to variation

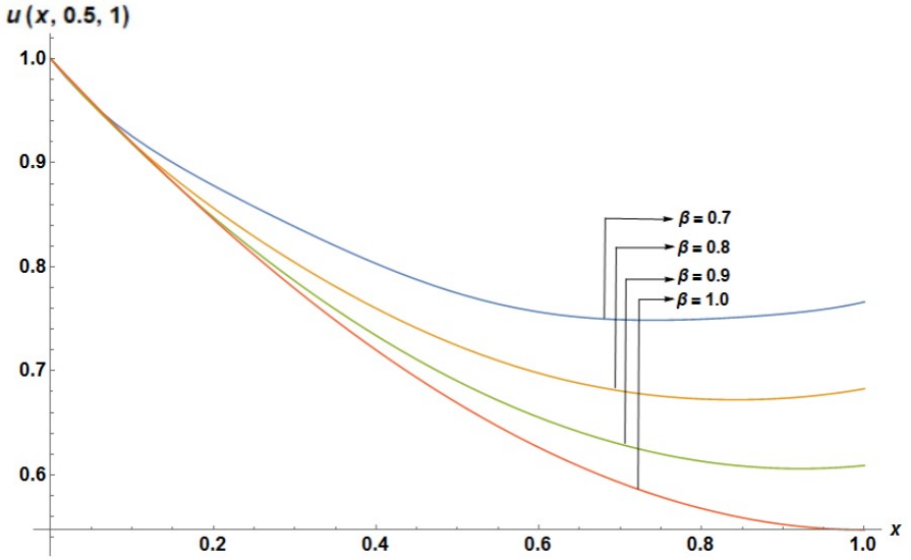

Figure 3.3: Plots of solute concentration at fixed $t = 1$ for $\alpha = 0.8$, $\beta = 0.7, 0.8, 0.9, 1.0$.

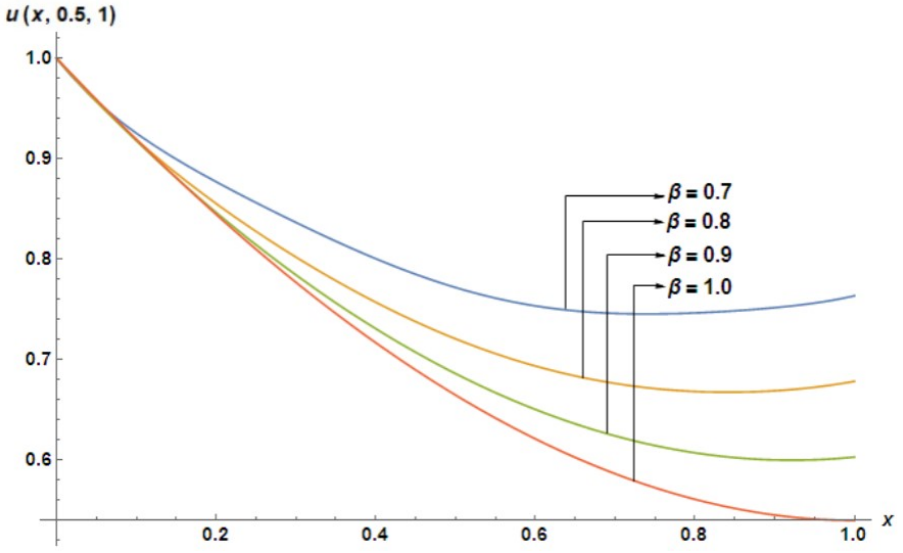

Figure 3.4: Plots of solute concentration at fixed $t = 1$ for $\alpha = 0.9$, $\beta = 0.7, 0.8, 0.9, 1.0$.

of $\beta = 0.7, 0.8, 0.9, 1.0$ at fixed $t = 1$ and $\alpha = 0.8$, while Figure 3.4 represents the movement of solute concentration due to variation of $\beta = 0.7, 0.8, 0.9, 1.0$ at fixed $t = 1$ and $\alpha = 0.9$, and Figure 3.5 represents the movement of solute concentration for $\beta = 0.7, 0.8, 0.9, 1.0$ at fixed $t = 1$ and $\alpha = 1.0$. Hence from Figures 3.3, 3.4 and 3.5, it is observed that for a fixed α the concentration of solution increases as β

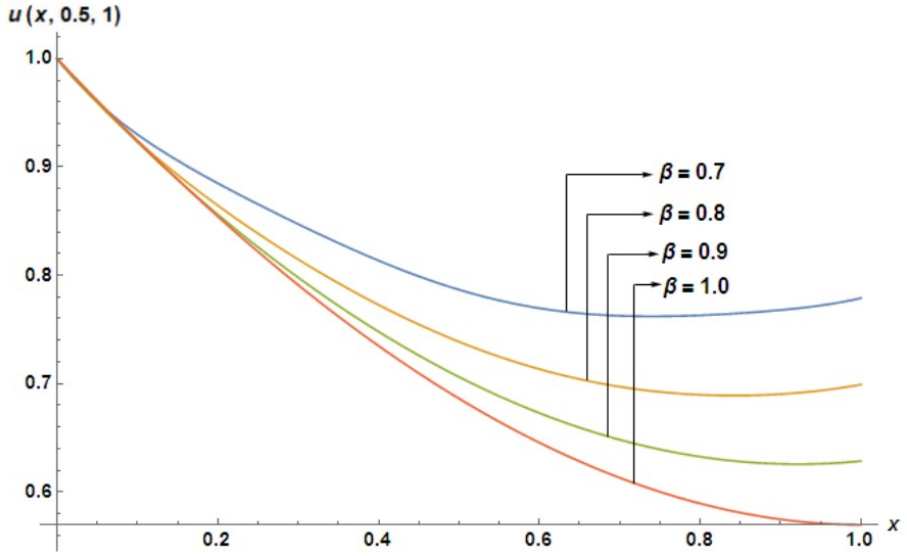

Figure 3.5: Plots of solute concentration at fixed $t = 1$ for $\alpha = 1.0$, $\beta = 0.7, 0.8, 0.9, 1.0$.

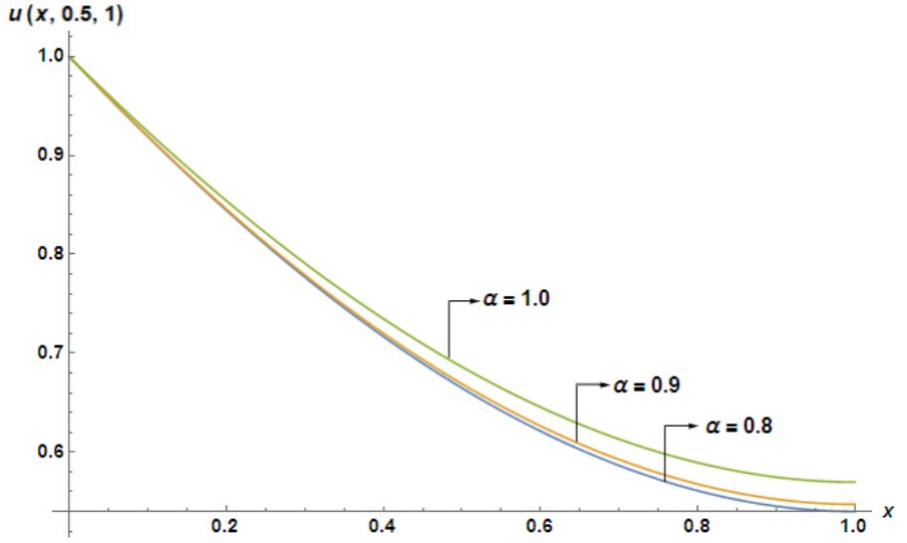

Figure 3.6: Plots of concentration of solution at fixed $t = 1$ for $\beta = 1.0$, $\alpha = 0.8, 0.9, 1.0$.

varies from integer order to fractional order. In each case it is found that as β (the order of spatial derivative) decreases, the solute concentration increases.

Figure 3.6 is the plot of the movement of solute concentration for $\alpha = 0.8, 0.9, 1.0$ at fixed $t = 1$ and $\beta = 1.0$. Hence it is observed that for a fixed $\beta = 1.0$, the solute concentration decreases as α varies from integer order to fractional order. These

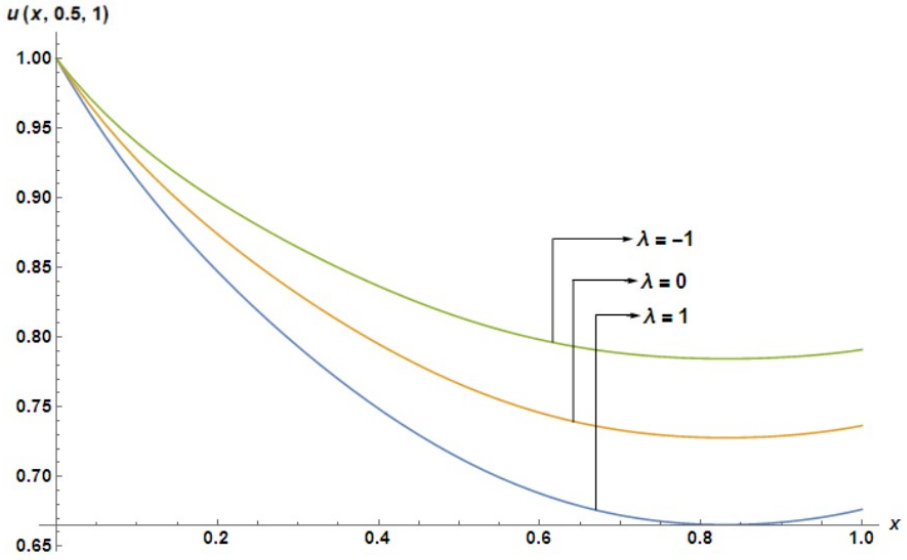

Figure 3.7: Plots of concentration of solution at fixed $t = 1$ for $\alpha = 0.8$, $\beta = 0.8, \nu_1 = 0.3, \nu_2 = 0.6, D = 1$ and $\lambda = -1, 0, 1$.

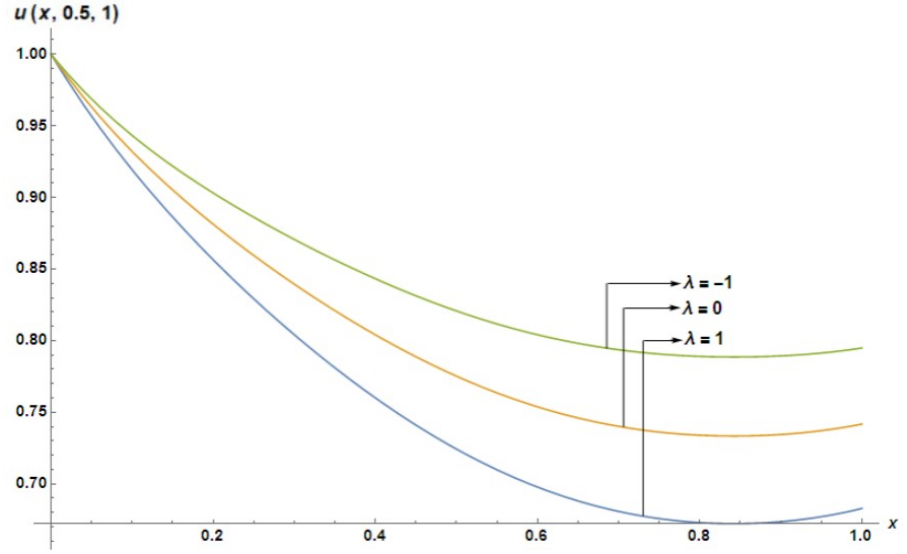

Figure 3.8: Plots of solute concentration at fixed $t = 1$ for $\alpha = 0.8$, $\beta = 0.8, \nu_1 = 0.6, \nu_2 = 0.3, D = 1$ and $\lambda = -1, 0, 1$.

results demonstrate not only the role of the order of the derivatives in describing effectively the pollutant transport in porous media, but also the need to employ the FRADE instead of RADE to study the fate of pollutant transportation in such systems.

Figure 3.7 shows the variations of solute concentration at $\beta = 0.8 = \alpha$, $\nu_1 = 0.3$,

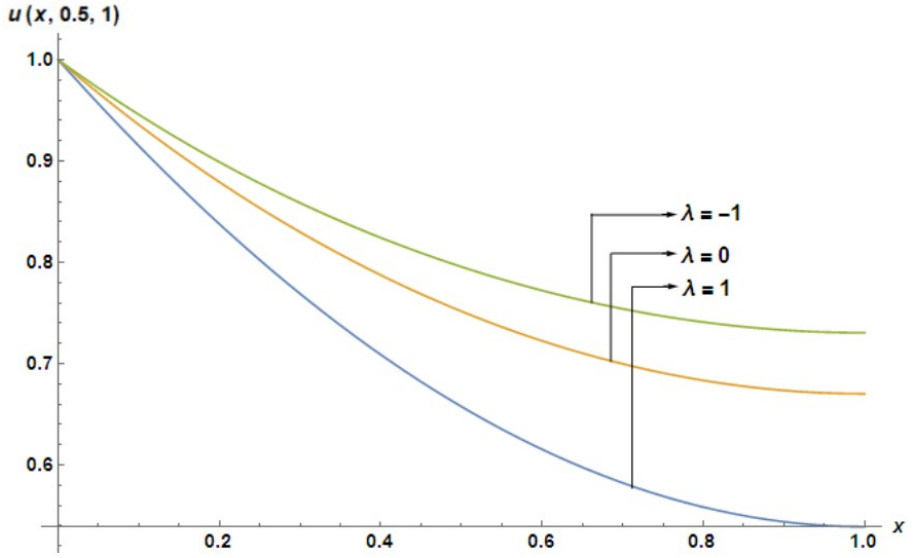

Figure 3.9: Plots of solute concentration at fixed $t = 1$ for $\alpha = 1.0$, $\beta = 1.0$, $\nu_1 = 0.3, \nu_2 = 0.6$, $D = 1$ and $\lambda = -1, 0, 1$.

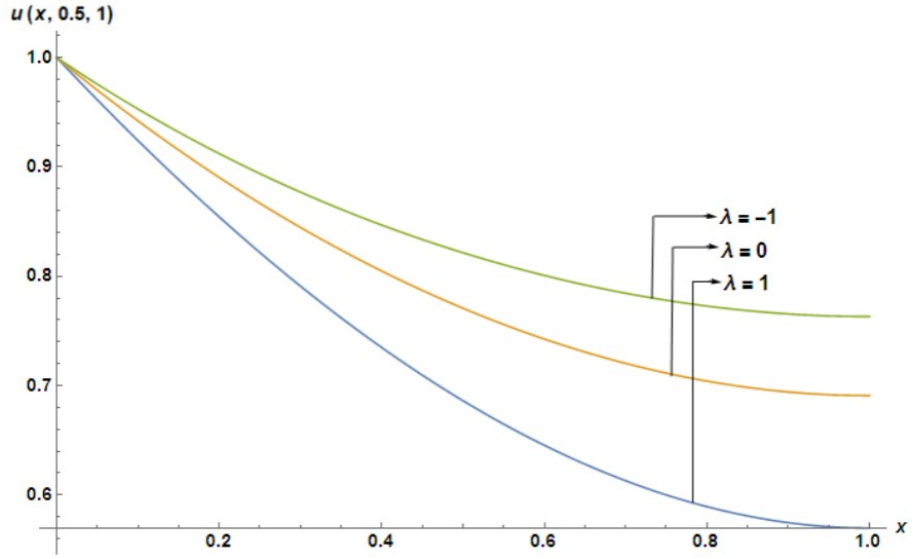

Figure 3.10: Plots of solute concentration at fixed $t = 1$ for $\alpha = 1.0$, $\beta = 1.0$, $\nu_1 = 0.6, \nu_2 = 0.3$, $D = 1$ and $\lambda = -1, 0, 1$.

$\nu_2 = 0.6$, $D = 1$, $t = 1$ for the values $\lambda = -1, 0, 1$. Figure 3.8 represents the variation of solute concentration at $\beta = 0.8 = \alpha$, $\nu_1 = 0.6$, $\nu_2 = 0.3$, $D = 1$, $t = 1$ for $\lambda = -1, 0, 1$. Figure 3.9 represents the plots of solute concentration at $\beta = 1.0 = \alpha$, $\nu_1 = 0.3$, $\nu_2 = 0.6$, $D = 1$, $t = 1$ for $\lambda = -1, 0, 1$. Figure 3.10 represents the plots of solute concentration at $\beta = 1.0 = \alpha$, $\nu_1 = 0.6$, $\nu_2 = 0.3$, $D = 1$, $t = 1$ for

$\lambda = -1, 0, 1$. Hence from Figures 3.7, 3.8, 3.9 and 3.10, it is observed that for a fixed value of α and β, the solute concentration is less for the system with sink term ($\lambda = 1$), as compared to the system with conservative contaminant ($\lambda = 0$), and for the system with source term ($\lambda = -1$). This is physically justified that more damping will be found in the presence of sink term ($\lambda = 1$) as compared to the source term ($\lambda = -1$) as well as for the case of conservative system ($\lambda = 0$).

3.4 Conclusion

In the present scientific contribution, the nonlinear space-time fractional-order RADE problem is solved by using a numerical method known as the shifted Legendre collocation method with the help of the operational matrices for derivatives. The accuracy and efficiency of the method are confirmed through error analyses of the results obtained between the proposed approach and the existing analytical method. Then, the proposed methodology is employed to solve the contaminant transport in groundwater problem defined by FRADE. For variations in space and time, the effect caused by the advection term on the solution profile are visually shown along with the impact of order of the spatial and time derivatives on the solution profile. Another focus of the research is the explanation of the damping of the solution profile as the system approaches to fractional order from standard order. The current contribution will be useful to scientists and engineers working in the field of transport in porous media.

****